Band structure in the $N=88$ isotones ^{149}Pm, ^{151}Eu, and ^{153}Tb

S. Bhattacharya and S. Sen
Saha Institute of Nuclear Physics, Calcutta-700 009, India

R. K. Guchhait
Department of Physics, Gurudas College, Calcutta-700 054, India
(Received 20 March 1985)

A particle-rotor model which incorporates the variable moment of inertia formalism is applied to the $N=88$ transitional nuclei, ^{149}Pm, ^{151}Eu, and ^{153}Tb. The model with a few adjustable parameters gives a very good account of the $\Delta I=1$, "normal" and $\Delta I=2$ "decoupled" band-like structures observed in these nuclei. The calculated level structure, single-nucleon-transfer spectroscopic factors, electromagnetic transition strengths, and relative gamma-ray branching are compared with available experimental data and predictions of other theoretical calculations.

I. INTRODUCTION

The study of the excitation modes of the transitional nuclei has evoked considerable interest for a long time. These nuclei are known to exhibit appreciable collectivity in their level properties. However, the nature of collectivity is not very clear in the sense that some of these properties correspond to those of "spherical" nuclei and some correspond to those of "deformed" nuclei. Recent experimental studies on a number of odd-A nuclei in the transitional regions which were normally considered as spherical have shown the existence of "normal" ($\Delta I=1$) and "decoupled" band ($\Delta I=2$) like structures in their excitation spectra. The nuclei ^{149}Pm, ^{151}Eu, and ^{153}Tb with 88 neutrons are situated in a region of the Periodic Table where the transition from spherical to permanently deformed shape is observed as the neutron number changes from 88 to 90. While the low-lying levels of the neighboring heavier isotopes ^{151}Pm, ^{153}Eu, and ^{155}Tb were known to have clear rotational structure, these nuclei were believed to be predominantly spherical. However, recent experimental investigations have revealed the existence of normal ($\Delta I=1$) positive parity bands based on $d_{5/2}$ and $g_{7/2}$ orbitals and a decoupled ($\Delta I=2$) negative parity band based on the $h_{11/2}$ orbital in these nuclei. A comprehensive list of experimental work on these isotopes can be found in Refs. 1 and 2. Of these three isotones, the nucleus ^{151}Eu has drawn considerable attention from both experimental and theoretical workers because of the fact that it is the only stable $N=88$ nucleus. The level structure of this isotope has been studied in the framework of a quasiparticle-anharmonic-vibration coupling model[1] as well as in a simple version of the particle-rotor coupling model.[3,4] Not surprisingly both the models seem to be partially successful in explaining the observed level properties; particularly the former model[1] is found to give a very good account of the $B(E2)$ values for a large number of excited levels measured in the Coulomb excitation experiment.[4] The isotope has also been studied in the interacting-boson-fermion model (IBFM) and the agreement between the calculated and the observed level energies is found to be very good.[5,6] The quasiparticle anharmonic vibration model referred to above is also found to reproduce more or less correctly the level energies and fragmentation of the $l=2$, 4, and 5 single particle strengths below 1.5 MeV excitation energies in the isotopes ^{149}Pm and ^{153}Tb. However, this model fails to predict the observed high-spin positive and negative parity band members as well as the antialigned low spin negative parity states based on the $h_{11/2}$ orbital. The ground state bands of the neighboring even nuclei are well described by the variable moment of inertia (VMI) formalism of Mariscotti *et al.*[7] Voklov[8] and also Gregory and Taylor[9] have shown that, when Coriolis effects can be ignored, a direct extension of the VMI model from the even-even cores to their adjacent odd-A partners gives reasonable results for the odd-A band energies. Smith, Rickey, and Simms[10] have shown that a Coriolis coupling model which incorporates the VMI approach with suitable modifications for odd-A nuclei can explain a wide range of phenomena observed in transitional nuclei. The model is simple with a small number of adjustable parameters. The aim of the present work is to see how far this model is able to reproduce the wide variety of experimental observations in these $N=88$ transitional nuclei in a systematic way. Preliminary results of the calculation on the negative parity band structure in these isotones have been reported elsewhere.[11] Since this model has been discussed in detail by Smith, Rickey, and Simms,[10] we shall briefly discuss the formalism and mainly concentrate on the results of the calculation.

II. THE MODEL

The model is based on the assumption that the nuclei under consideration are axially symmetric and have a reflection symmetry with respect to a plane perpendicular to the symmetry axis. The calculations are carried out within the framework of a simple model where the motion of an unpaired quasiparticle moving in Nilsson's deformed orbit is coupled to the rotational motion through the Coriolis interaction.

The total Hamiltonian is taken as

$$H = H_p + H_{\rm rot} \ , \tag{1}$$

where H_p is the usual single particle deformed shell model Hamiltonian with energy eigenvalue e_K, transformed into quasiparticle energies according to

$$E_{K,\nu} = [(e_{K,\nu} - \lambda)^2 + \Delta^2]^{1/2} - \Delta \tag{2}$$

and

$$H_{\rm rot} = \frac{\hbar^2}{2\mathscr{I}}(I - j)^2 = \frac{\hbar^2}{2\mathscr{I}}[I^2 + j^2 - 2I_3 j_3 - (I_+ j_- + I_- j_+)] \ . \tag{3}$$

The last term is the so-called Coriolis term, and the components of j and I are with respect to the nuclear body fixed axes, the 3-axis being the symmetry axis.

In the absence of the Coriolis coupling, the total wave function $|IMK\rangle$ is given by[12]

$$|IMK\nu\rangle = \left[\frac{2I+1}{16\pi^2}\right]^{1/2} [D^I_{M,K}\chi_{K,\nu} + (-)^{I+K} D^I_{M,-K}\chi_{-K,\nu}] \ , \tag{4}$$

where

$$\chi_{-K,\nu} = \sum_j (-)^{j+K} C_{j,K,\nu} |j, -K\rangle \ . \tag{5}$$

The total Hamiltonian can be rewritten as

$$H = H_p + H_{\rm rot} = H_0 + H_{\rm cor} \ , \tag{6}$$

where

$$H_0 = H_p + \frac{\hbar^2}{2\mathscr{I}}(I^2 + j^2 - 2I_3 j_3) \tag{7a}$$

and

$$H_{\rm cor} = -\frac{\hbar^2}{2\mathscr{I}}(I_+ j_- + I_- j_+) \ . \tag{7b}$$

The diagonal element of the Hamiltonian (6) is expressed as

$$\langle H\rangle_{\rm dia} = E_{K,\nu} + \frac{\hbar^2}{2\mathscr{I}}[I(I+1) + \langle j^2\rangle - 2K^2 + \delta_{K,1/2} a (-)^{I+(1/2)}(I+\tfrac{1}{2})] \ , \tag{8}$$

where the decoupling parameter a and $\langle j^2\rangle$ are given by

$$a = -\sum_j (-)^{j+(1/2)}(j+\tfrac{1}{2}) c^2_{j,1/2} \ , \tag{9a}$$

and

$$\langle j^2\rangle = \sum_j C^2_{jK} j(j+1) \ . \tag{9b}$$

The off-diagonal matrix elements of the Coriolis interaction (7b) between the states of different rotational bands with $|\Delta K| = 1$ are given by

$$\langle IM\,K\pm1\,\nu'|H_{\rm cor}|IMK\nu\rangle = -\frac{\hbar^2}{2\mathscr{I}}(U_{K\pm1\nu'}U_{K\nu} + V_{K\pm1\nu'}V_{K\nu})[(I\mp K)(I\pm K+1)]^{1/2} \times \sum_j C_{j,\Omega,\nu} C_{j,\Omega\pm1,\nu'}[(j\mp\Omega)(j\pm\Omega+1)]^{1/2} \ . \tag{10}$$

The diagonalization leads to the Coriolis-mixed eigenfunctions

$$|IM\rangle = \sum_K f_{IK}[D^I_{M,K}\chi_K + (-)^{I+K} D^I_{M,-K}\chi_{-K}] \ , \tag{11}$$

where f_{IK}'s are determined through the diagonalization procedure. Instead of using a constant moment of inertia $\mathscr{I}$, an approach similar to that of Smith and Rickey[10] has been adopted to impose a realistic core behavior on the unperturbed odd-particle state based on the variable moment of inertia model of Mariscotti *et al.*[7] As a consequence, an "elastic energy" term $\frac{1}{2}C(\mathscr{I}_{IK} - \mathscr{I}_{0K})^2$ has been added to the diagonal term defined in Eq. (8) and the moment of inertia $\mathscr{I}_{IK}$ is calculated from the following expression:

$$\mathscr{I}_{IK} = \{(\tfrac{1}{2}C)[I(I+1) - 2K^2 + \langle j^2\rangle + \delta_{K,1/2} a (-)^{I+(1/2)}(I+\tfrac{1}{2})]\}^{1/3} \ , \tag{12}$$

where C has been treated as a free parameter and $\mathscr{I}_{0K}$ is calculated from the expression (12) by putting $\mathscr{I}_{0K} = \mathscr{I}_{IK}$ $(I = j_0)$, where j_0 is the angular momentum of the spherical shell model state to which the state $|IMK\rangle$ degenerates at zero deformation. The moment of inertia parameter, A_{IK} $(= 1/2\mathscr{I}_{IK})$, which appears as the energy scale factor in the Coriolis matrix element [Eq. (10)], was set equal to the average value of A_{IK} and $A_{IK'}$.

The single nucleon-transfer spectroscopic factors for stripping reactions and the fraction of the state $|IM\rangle$ which contains the core angular moment $R = R_0, P(IM, R_0)$ are calculated in the standard way.[10] The static and dynamic moments of the electromagnetic transition operators ($E2$ and $M1$) between different states have been calculated following the procedure described by Bohr and Mottelson.[12]

III. PARAMETERS OF THE CALCULATION

The Nilsson single-particle levels appropriate for odd-proton nuclei in this mass region were calculated by adjusting the shell model parameters κ and μ in a way so that the $d_{5/2}$, $g_{7/2}$, $s_{1/2}$, $d_{3/2}$, and $h_{11/2}$ level energies at zero deformation corresponded to those determined by Reehal and Sorensen.[13] The values of μ and κ thus obtained were 0.59 and 0.05, respectively. It was found that however accurately we tried to determine these parameters through the above-mentioned procedure, some adjustment in the single-particle energies of one or two levels (of the

order of a few hundred keV) were necessary to reproduce the low energy part of the spectrum in each isotone. These adjustments in the single-particle energies were found to be minimal if the values of μ and κ were taken as 0.50 and 0.05, respectively. Therefore, we proceeded with these values of μ and κ for all the isotones under consideration. Similar adjustments were found necessary by other workers also.[10,14] The deformation parameter δ was taken to be $\delta=0.14$ for all the nuclei. In the quasirotational picture, the deformation parameter can be determined from the measured $B(E2\ 0^+\rightarrow 2^+)$ values in the neighboring even-even isotopes. The values of δ determined for ^{148}Nd, ^{150}Sm, and ^{152}Gd lie in the range $\delta=0.14$–0.18. The pairing gap and the Fermi level parameters Δ and λ were determined through the solution of the gap equation in each case with a value of strength parameter $G=27/A$. All the Nilsson orbitals arising from the $1g_{9/2}$, $1g_{7/2}$, $2d_{5/2}$, $2d_{3/2}$, $3s_{1/2}$, and $1h_{11/2}$ shell model states were used in the calculation. The variable moment of inertia parameter C was taken to be 1.0×10^7 and 0.3×10^7 keV^3 for the negative and positive parity states, respectively. Finally the Coriolis matrix elements (including the decoupling term) had to be reduced to 80% and 85% of its theoretical value for the calculation of the positive and negative parity states, respectively. This latter adjustment is usually necessary in the rare-earth region where Coriolis matrix elements are found to be significantly smaller than their theoretical estimate.[10]

The $M1$ moments and transition rates were calculated with $g_l=1.0$, $(g_s)_{\rm eff}=3.5$, and $g_R=Z/A$. We tried to restrict the adjustment of different parameters to the minimum as our main motive was to see how far this model could explain the observed properties of these nuclei in a systematic way with a parameter set common to all of them except, of course, the values of $\hbar\omega_0(\delta)$, λ, and Δ which vary with mass number. Plots of the effective moment of inertia parameters A_{IK}'s for different values of the spins and band quantum numbers are presented in Figs. 1 and 2. The spin dependence of $\mathscr{I}_I$ is seen to be monotonic in all bands except the $K=\frac{1}{2}$ bands, where the presence of the diagonal Coriolis term [Eq. (12)] induces oscillations in $\mathscr{I}$ with spin. This oscillation is not prominent for the $K=\frac{1}{2}$ band arising from the $d_{5/2}$ orbital because of the small value of the decoupling coefficient parameter for this band. This oscillation is essential to the success of the present calculation in correctly reproducing the excitation energies of the high spin negative parity states; a constant or monotonically increasing $\mathscr{I}$ in the $K=\frac{1}{2}$ bands does not reproduce the $\Delta I=2$ decoupled bandlike structure observed in these isotones.

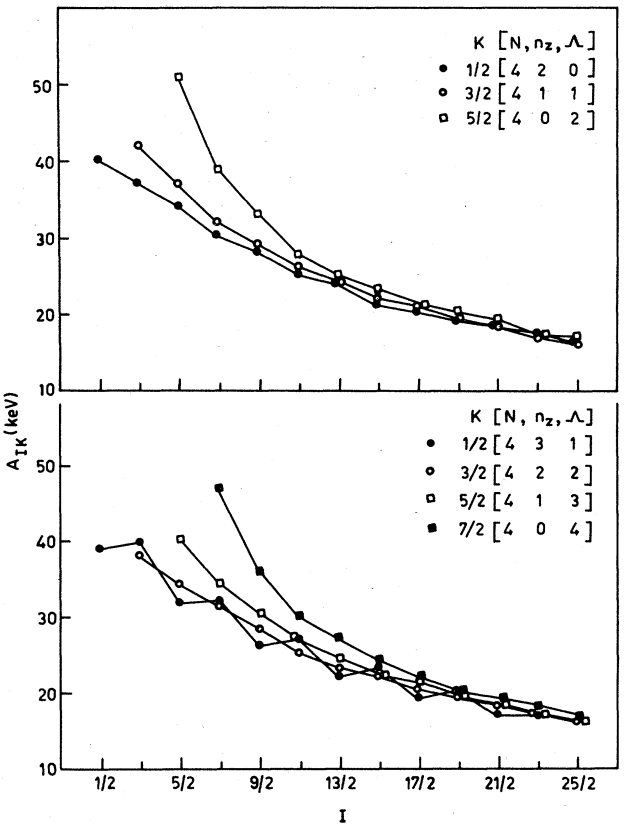

FIG. 1. Semiempirical moment of inertia parameters for the odd-proton Nilsson states whose parentage is the $d_{5/2}$ and $g_{7/2}$ spherical shell-model states. These states are listed in the figure according to the asymptotic quantum numbers.

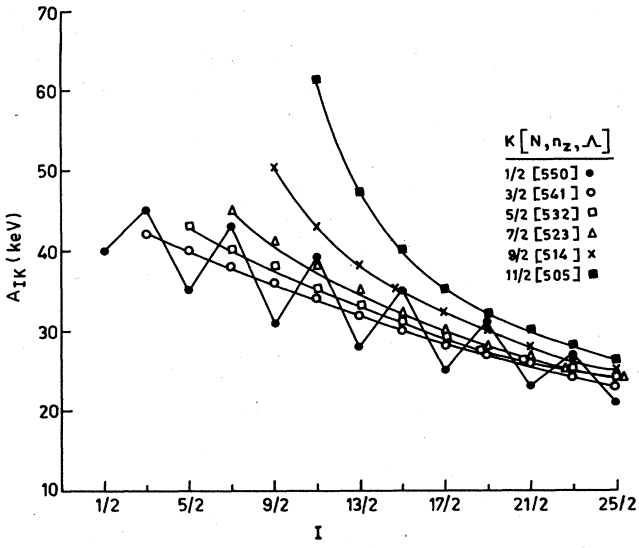

FIG. 2. Semiempirical moment of inertia parameters for the odd-proton Nilsson states whose parentage is the $h_{11/2}$ spherical shell-model states. These states are listed in the figure according to the asymptotic quantum numbers.

IV. NEGATIVE PARITY STATES

The nuclei ^{151}Eu and ^{153}Tb show a definite $\Delta I=2$ band of "favored" states based on an $\frac{11}{2}^-$ state and the character of this band in these nuclei is essentially the same.[2,15,16] In ^{149}Pm, this band structure has not been established in detail. Moreover, several low spin states ($\frac{3}{2}^-$, $\frac{5}{2}^-$, and $\frac{7}{2}^-$) have been observed in the low energy spectra of these nuclei.[2,15–17] In ^{153}Tb, negative parity states having spin values from $\frac{3}{2}$ to $\frac{35}{2}$ have been observed.[2] Thus

the negative parity states in these nuclei provide a very good test for the rotational description of these nuclei. The negative parity state calculations were carried out including in the basis all the Nilsson states arising from the $h_{11/2}$ orbital. The negative-parity calculations agree quite well with experiment (Figs. 3–5). The angular momenta of the states forming the $\Delta I=2$ decoupled band based on the $h_{11/2}$ orbital appear to be the result of an alignment of the particle (j) and the core (R) angular momentum ($I=j+R$). This simple picture is consistent with the detailed calculation as is evident from the calculated wave functions and the $P(IM,R_0)$ factors of the states in ^{153}Tb listed in Tables I and II, respectively. First, it is seen that the states identified as rotation aligned ($\frac{11}{2}^-$, $\frac{15}{2}^-$, $\frac{19}{2}^-$, etc.) are mainly based on the $K=\frac{1}{2}$ and $\frac{3}{2}$ bands (i.e., the projection of j on the nuclear symmetry axis is minimal, so j and R are maximally aligned). The dominant R components of these states also show this rotation alignment nature, i.e., the band head, ($\frac{11}{2}^-$) is calculated to be primarily $R=0$, the first rotational state ($\frac{15}{2}^-$), $R=2$, etc. So far as the electromagnetic properties of these states are concerned, the present calculation predicts an enhancement of the $B(E2)$ rates by a factor of 30–35 times the single particle estimates. Since the dominant components of these states come from the same Nilsson bands ($K=\frac{1}{2},\frac{3}{2}$), transitions between these states are "intraband" and they are expected to be enhanced. This seems to be consistent with the decay modes of these levels (Table III).

The identification of the antialigned states ($\frac{7}{2}^-$, $\frac{3}{2}^-$, etc.) is also evident from Tables I and II. These states also predominantly arise from the $K=\frac{1}{2}$ and $\frac{3}{2}$ orbitals

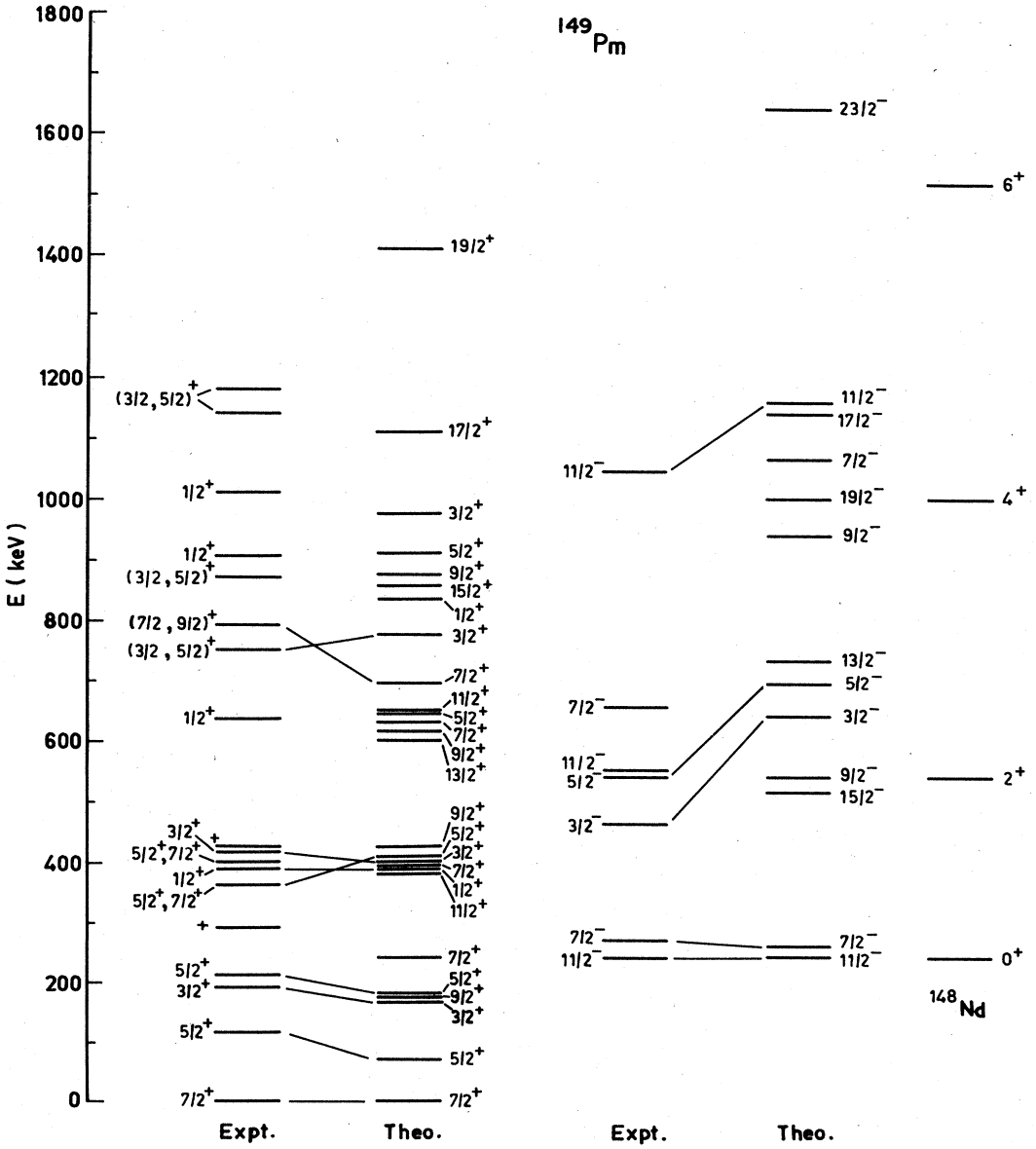

FIG. 3. Calculated and experimental (Refs. 17 and 18) energy spectra in ^{149}Pm.

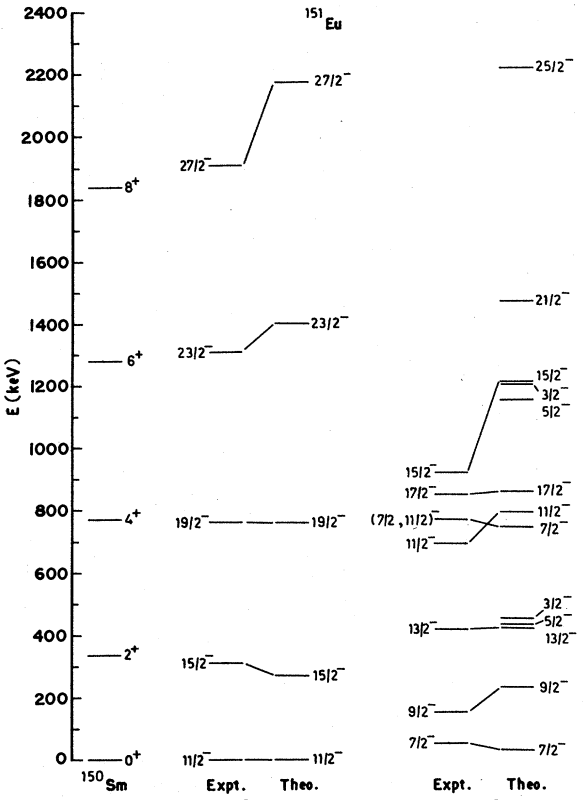

FIG. 4. Summary of the experimental (Refs. 3–5 and 16–18) and theoretical results for the negative-parity states in ^{151}Eu. Also shown for comparison are the ground state bands of the adjacent even-even ^{150}Sm core. The excitation energies of the negative parity states are relative to the $\frac{11}{2}^-$ state at 0.196 MeV. The states forming the decoupled band are shown separately.

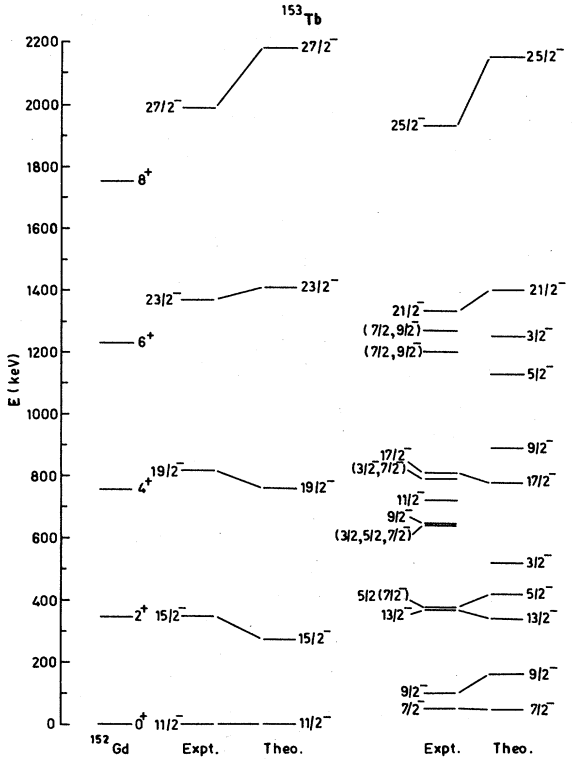

FIG. 5. Summary of the experimental (Ref. 2) and theoretical results for the negative-parity states in ^{153}Tb. Also shown for comparison are the ground-state bands of the adjacent even-even ^{152}Gd core. The excitation energies of the negative parity states are relative to the $\frac{11}{2}^-$ state at 0.163 MeV. The states forming the decoupled band are shown separately.

and have the expected major R components, except in this case $I=|j-R|$. The low spin negative parity states $\frac{3}{2}^-$ and $\frac{5}{2}^-$ have been experimentally observed in ^{149}Pm at 462 and 538 keV, respectively.[17] The present calculation is successful in reproducing these states. Although the calculated $\frac{3}{2}^-$ and $\frac{5}{2}^-$ states lie at higher energy than their experimental values, the agreement becomes much better if we use a value of $C=0.5\times10^7$ keV^3. Since not many negative parity states have been experimentally identified in ^{149}Pm and our main interest was to study the overall systematics in these isotones, the calculations were carried out with the same value of C, viz., 1.0×10^7, for all the isotones. In ^{153}Tb also, several low-spin negative parity states ($\frac{3}{2}^-$, $\frac{5}{2}^-$, and $\frac{7}{2}^-$) have been identified.[2] From energy consideration the 537, 624, and 707 or 800 keV states can be identified with the calculated $\frac{5}{2}^-$ state at 581, $\frac{3}{2}^-$ state at 680, and $\frac{7}{2}^-$ state at 822 keV, respectively (Fig. 5). No such low-spin negative parity states have so far been identified in ^{151}Eu. The present calculation is also equally successful in reproducing the excitation energies of several other "unfavored" high spin states ($\frac{13}{2}^-$, $\frac{17}{2}^-$, $\frac{21}{2}^-$, and $\frac{25}{2}^-$ states). From the present calculation it appears that the rotation alignment becomes more and more complete as the proton number decreases from $Z=65$ (Tb isotope) to $Z=61$ (Pm isotope). This becomes evident if one compares the relative excitation energies of the rotation aligned states in the odd-mass isotopes with those of the corresponding even-even core states (Figs. 3–5). This feature is reflected in the compositions of the favored states in these nuclei. The low K orbitals, $K=\frac{1}{2}$ and $\frac{3}{2}$, contribute about 80%, 70%, and 60% to the wave functions of these states in ^{149}Pm, ^{151}Eu, and ^{153}Tb, respectively. A search for the location of the high spin negative parity states in ^{149}Pm through heavy ion reaction studies would be useful in testing this theoretical prediction.

The spectroscopic factors for the stripping reaction to the $\frac{11}{2}^-$ states in ^{149}Pm, ^{151}Eu, and ^{153}Tb have been calculated and they are found to be in good agreement with the experimental results (Table IV). However, the magnetic moment of the 270 keV $\frac{7}{2}^-$ state in ^{149}Pm is not correctly reproduced (Table V). In view of the large fluctuations in the results of different experimental measurements[17] on the magnetic moments of both positive and negative parity states in ^{149}Pm, it is difficult to make a useful comment on this disagreement. Since the magnetic moments provide a stringent test of the correctness of calculated wave functions, it would be worthwhile to undertake more accurate measurements of the magnetic moments of these levels in ^{149}Pm. In summary, the present calculation is

TABLE I. Experimental and calculated energies and wave functions for the negative parity states in ^{153}Tb.

States	I^π	E (keV) Expt.[a]	Calc.	$\frac{1}{2}[550]$	$\frac{3}{2}[541]$	$\frac{5}{2}[532]$	$\frac{7}{2}[523]$	$\frac{5}{2}[514]$	$\frac{11}{2}[505]$
Rotation aligned	$\frac{11}{2}^-$	163	163	0.520	0.593	0.513	0.315	0.124	0.029
	$\frac{15}{2}^-$	511.4	437	0.532	0.595	0.503	0.307	0.124	0.029
	$\frac{19}{2}^-$	978.9	926	0.544	0.599	0.495	0.295	0.116	0.026
	$\frac{23}{2}^-$	1532.9	1572	0.552	0.602	0.489	0.285	0.110	0.024
	$\frac{27}{2}^-$	2155.6	2345	0.557	0.604	0.485	0.278	0.105	0.022
Rotation antialigned	$\frac{7}{2}^-$	213.8	207	0.551	0.620	0.504	0.242		
	$\frac{3}{2}^-$	625[b]	680	0.757	0.653				
Other states	$\frac{11}{2}^-$	883	845	−0.510	−0.248	0.318	0.611	0.426	0.149
	$\frac{9}{2}^-$	263	326	0.208	0.525	0.654	0.470	0.180	
	$\frac{13}{2}^-$	535.6	504	0.199	0.509	0.639	0.487	0.227	0.060
	$\frac{17}{2}^-$	966.9	945	0.203	0.520	0.639	0.478	0.220	0.056
	$\frac{21}{2}^-$	1495.0	1560	0.208	0.532	0.639	0.468	0.210	0.051
	$\frac{25}{2}^-$	2095.1	2309	0.211	0.541	0.639	0.459	0.201	0.048

[a] Reference 2.
[b] This level is tentatively given an $l=1,2$ assignment in (^{3}He,d) and (d,t) experiments (Ref. 18).

successful in reproducing the observed excitation energies of the negative parity states having spin values from $\frac{3}{2}$ to $\frac{27}{2}$ as well as the spectroscopic strengths of the $\frac{11}{2}^-$ levels.

V. POSITIVE PARITY STATES

Positive parity states having spin values from $I=\frac{1}{2}$ to $\frac{27}{2}$ have been identified in ^{153}Tb through decay and (α,xn) reaction studies.[2] In ^{151}Eu, although the highest spin value for the positive parity states identified so far is $\frac{17}{2}^+$, the $B(E2)\uparrow$ transition rates for a large number of low-lying states is known through Coulomb excitation work.[4] In ^{149}Pm, several low spin positive parity states ($I\leq\frac{7}{2}$) are known through decay work.[17] Although some of the positive parity states in ^{151}Eu and ^{153}Tb have been identified with $\frac{5}{2}[402]$, $\frac{5}{2}[413]$, and $\frac{7}{2}[404]$ Nilsson states, the band structures are not so well developed. The high-spin positive parity states appear to form a $\Delta I=1$ normal

TABLE II. Calculated rotational compositions for the negative parity states in ^{153}Tb.

State	I^π	E (keV)$_{\text{Calc.}}$	$P(IM,R_0)$ $R_0=0$	2	4	6	8
Rotation aligned	$\frac{11}{2}^-$	163	0.692	0.289	0.005	0.011	0.003
	$\frac{15}{2}^-$	437	0.0	0.874	0.110	0.006	0.008
	$\frac{19}{2}^-$	926	0.0	0.0	0.906	0.078	0.008
	$\frac{23}{2}^-$	1572	0.0	0.0	0.0	0.916	0.067
	$\frac{27}{2}^-$	2345	0.0	0.0	0.0	0.0	0.920
Rotation antialigned	$\frac{7}{2}^-$	207	0.046	0.94	0.0	0.012	0.001
	$\frac{3}{2}^-$	680	0.002	0.073	0.912	0.013	0.0
Others	$\frac{9}{2}^-$	326	0.003	0.775	0.219	0.002	0.0
	$\frac{13}{2}^-$	504	0.0	0.597	0.370	0.033	0.0
	$\frac{17}{2}^-$	945	0.0	0.0	0.749	0.239	0.012
	$\frac{21}{2}^-$	1560	0.0	0.0	0.0	0.808	0.184
	$\frac{25}{2}^-$	2309	0.0	0.0	0.0	0.0	0.838

TABLE III. Calculated and experimental decay modes and partial γ half-lives of a few levels in ^{149}Pm, ^{151}Eu, and ^{153}Tb. Excitation energies are given in keV. The numbers listed under $T(E2)$ and $T(M1)$ are to be multiplied by powers of ten given in the parentheses.

	Initial	Final			δ^2		Branching ratio		Half-life (nsec)	
A	state	state	$T(E2)$ sec^{-1}	$T(M1)$ sec^{-1}	Calc.	Expt.[a]	Calc.	Expt.[a]	Calc.	Expt.
^{149}Pm	114($\frac{5}{2}^+$)	0($\frac{7}{2}^+$)	1.91(7)	9.2(7)	0.208				6.25	5.0[b]
	211($\frac{5}{2}^+$)	0($\frac{7}{2}^+$)	3.63(8)	4.14(9)	0.088		1	1	0.15	0.09[b]
		114($\frac{5}{2}^+$)	2.44(5)	8.46(7)	0.003		0.02	0.05		
	188($\frac{3}{2}^+$)	0($\frac{7}{2}^+$)	3.55(7)				1	1	5.85	4.0[b]
		114($\frac{5}{2}^+$)	5.73(6)	7.8(7)	0.075		2.3	0.65		
	360($\frac{5}{2}^+$)	0($\frac{7}{2}^+$)	3.87(8)	6.69(7)	5.78		0.033	0.16		
		114($\frac{5}{2}^+$)	1.26(9)	1.02(10)	0.123		1.0	1.0		
^{151}Eu	22($\frac{7}{2}^+$)	0($\frac{5}{2}^+$)	3.3(3)	4.8(5)	0.007	0.001			1400	241[b]
	196($\frac{3}{2}^+$)	0($\frac{5}{2}^+$)	1.56(8)	4.51(9)	0.034				0.15	0.33[b]
^{153}Tb	81($\frac{7}{2}^+$)	0($\frac{5}{2}^+$)	6.0(6)	3.13(8)	0.019	0.012			2.2	1.8[c]
	147($\frac{3}{2}^+$)	0($\frac{5}{2}^+$)	1.09(6)	3.95(9)	0.0003	0.20			0.18	1.25[c]
	263($\frac{9}{2}^-$)	163($\frac{11}{2}^-$)	2.1(7)	2.55(9)	0.008	0.025			0.27	0.57[c]
	254($\frac{7}{2}^+$)	0($\frac{5}{2}^+$)	2.45(9)	4.69(10)	0.052		4.0	23.8		
		81($\frac{7}{2}^+$)	1.69(8)	1.22(10)	0.014		1.0	1.0		
	325($\frac{9}{2}^+$)	254($\frac{7}{2}^+$)	5.0(3)	1.42(8)			1.0	1.0		
		0($\frac{5}{2}^+$)	2.79(9)				19.6	9.0		
	529($\frac{11}{2}^+$)	325($\frac{9}{2}^+$)	1.1(9)	1.3(10)	0.085		1.0	1.0		
		81($\frac{7}{2}^+$)	3.03(10)				2.15	3.71		
	631($\frac{11}{2}^+$)	445($\frac{9}{2}^+$)	6.51(8)	2.19(10)	0.03		1.0	1.0		
		325($\frac{9}{2}^+$)	1.46(8)	3.03(10)	0.005		1.38	1.67		
		254($\frac{7}{2}^+$)	1.34(10)				1.61	2.2		
	755($\frac{13}{2}^+$)	325($\frac{9}{2}^+$)	3.78(10)				1.0	1.0		
		445($\frac{9}{2}^+$)	1.23(8)				0.003	0.069		
		529($\frac{11}{2}^+$)	2.59(9)	2.1(10)	0.123		0.55	0.425		
	1495($\frac{21}{2}^-$)	967($\frac{17}{2}^-$)	1.74(11)				7.7	1.6		
		979($\frac{19}{2}^-$)	2.2(10)	8.0(8)	27.5		1.0	1.0		
	967($\frac{17}{2}^-$)	535($\frac{13}{2}^-$)	5.9(10)				2.44	1.50		
		511($\frac{15}{2}^-$)	1.73(10)	6.94(9)	2.49		1.0	1.0		

[a] References 2 and 17.
[b] Partial gamma half-lives are calculated from the measured half-lives and the conversion coefficients (Ref. 17).
[c] Partial gamma half-lives are calculated from the measured half-lives and the conversion coefficients (Ref. 2).

band structure based most probably on $g_{7/2}$ and $d_{5/2}$ orbitals. In the negative parity calculation, j is an extremely good quantum number since all the six Nilsson states have almost 100% $h_{11/2}$ parentage, whereas, in the positive parity case, there is a significant amount of j mixing in the basis states. Because of the j mixing, the j is less prominent as a constant of motion of the odd particle than in the negative parity case. The positive-parity cal-

TABLE IV. Calculated and experimental spectroscopic factors.

A	I^π	E (keV)	$(2I+1)S$ Calc.	$(2I+1)S$ Expt.[a]
^{149}Pm	$\frac{7}{2}^+$	0	2.90	2.20
	$\frac{7}{2}^+$	789	0.21	0.74
	$\frac{5}{2}^+$	114	1.60	2.40
	$\frac{5}{2}^+$	211	0.74	0.06
	$\frac{3}{2}^+$	188	0	0.04
	$\frac{3}{2}^+$	414	0.82	0.78
	$\frac{3}{2}^+$	750	0.10	0.52
	$\frac{3}{2}^+$	871	0.06	0.44
	$\frac{11}{2}^-$	240	4.74	4.30
	$\frac{11}{2}^-$	1043	2.18	0.69
^{151}Eu	$\frac{7}{2}^+$	22	2.41	2.70
	$\frac{5}{2}^+$	0	1.80	2.40
	$\frac{5}{2}^+$	262	0.09	0.03
	$\frac{5}{2}^+$	307.2	0.21	0.47
	$\frac{3}{2}^+$	335	0.71	2.20
	$\frac{11}{2}^-$	197	4.39	6.40
	$\frac{11}{2}^-$	886	2.06	2.40
^{153}Tb	$\frac{7}{2}^+$	80	1.68	1.40
	$\frac{5}{2}^+$	0	1.54	1.90
	$\frac{5}{2}^+$	543	0.02	0.63
	$\frac{11}{2}^-$	163	5.42	6.20
	$\frac{11}{2}^-$	883	1.66	1.60

[a] Reference 18.

culations were performed including in the basis the Nilsson states $\frac{1}{2}[431]$, $\frac{1}{2}[420]$, $\frac{1}{2}[411]$, $\frac{3}{2}[422]$, $\frac{3}{2}[411]$, $\frac{5}{2}[413]$, $\frac{5}{2}[402]$, and $\frac{7}{2}[404]$. The spherical shell model state admixtures for these Nilsson states are presented in Table VI. The variation of the moment of inertia parameters A_{IK} with spin values, calculated using expression (12) and $C=0.3\times10^7$ keV^3 in the case of ^{153}Tb, is shown in Fig. 1.

As mentioned earlier, the single-particle energies of one or two levels had to be adjusted in each individual case by a few hundred keV in order to reproduce the low energy part of the spectrum. Otherwise, the only change made in going from ^{149}Pm to ^{153}Tb was in the mass number. Since the band structure is not so well developed, it is difficult to assign unambiguously most of the positive parity states to any particular band. The calculated wave functions (listed in Table VII for ^{153}Tb) show that the Coriolis interaction has introduced a significant amount of band mixing in the positive parity states. However, in some cases it is still possible to identify the states as members of a band based on a particular Nilsson orbital.

A. The nucleus ^{149}Pm

This isotope has been studied mainly through the decay of ^{149}Nd (Ref. 17) and the particle transfer reaction.[18,19] Available experimental data do not indicate the existence of any well defined band structure. The calculations were done by adjusting the single-particle energies of the $\frac{7}{2}[404]$ and $\frac{5}{2}[402]$ Nilsson orbitals by about 600 and 400 keV, respectively. The calculated level spectrum is found to be in good agreement with the experimental spectrum observed in the ^{149}Nd β-decay study (Fig. 3). The calculated $\frac{3}{2}^+$ state at 165 keV is identified with the 188 keV positive parity state in the experimental spectrum. The calculated lifetime and magnetic moment of the 165 keV state agree very well with the observed lifetime and magnetic moment of the 188 keV state (Tables III and V). On the basis of the similarity of the calculated and experimental decay modes and/or spectroscopic strengths, the 181 keV ($\frac{5}{2}^+$), 407 keV ($\frac{5}{2}^+$), 696 keV ($\frac{7}{2}^+$), 400 keV ($\frac{3}{2}^+$), 777 keV ($\frac{3}{2}^+$), and 976 keV ($\frac{3}{2}^+$) states in the theoretical spectrum are identified with the observed levels at 211, 360, 789, 414, 750, and 871 keV, respectively (Fig. 3). The calculated lifetimes of the $\frac{5}{2}^+_1$, $\frac{3}{2}^+_1$, and $\frac{5}{2}^+_2$ states are in very good agreement with the corresponding experimental value (Table III). The predicted magnetic moments of the $\frac{5}{2}^+_1$ and $\frac{7}{2}^+_1$ states differ by about 0.5 to 0.7 μ_N from their experimental values. There are four different measurements of the magnetic moment of the $\frac{5}{2}^+_1$ state and they differ considerably from each other. The measured magnetic moment of the $\frac{7}{2}^+_1$ state is also much higher than that of the $\frac{7}{2}^+_1$ state in ^{151}Eu (Table V). More accurate measurements of the magnetic moments of these states would be interesting. The calculated and experimental magnetic moments of the $\frac{5}{2}^+$ state at 211 keV agree quite well. The calculated spectroscopic strengths of some of the states are listed in Table IV along with their experimental values as obtained for the stripping reaction results of Straume *et al.*[18] The agreement can be considered to be reasonable.

B. The nucleus ^{151}Eu

In the calculation of the positive parity spectrum, the single particle energies of the $\frac{5}{2}[402]$ and the $\frac{7}{2}[404]$ bands had been adjusted by about 300 keV so that the quasiparticle energies of these two bands come down by about 150 keV. Four bands based on the $\frac{5}{2}[402]$, $\frac{7}{2}[404]$, $\frac{3}{2}[411]$, and $\frac{5}{2}[413]$ Nilsson orbitals can be identified in the calculated spectrum. The $\frac{5}{2}^+$ ground and the $\frac{7}{2}^+$ first excited states can be considered as the band heads based on the $\frac{5}{2}[402]$ and $\frac{7}{2}[404]$ Nilsson orbitals, respectively. The static electromagnetic moments of these states are known experimentally.[17,20] The calculated quadrupole moments for these states are in good agreement (Table V) with recent muonic x-ray results of Tanaka *et al.*[20] The magnetic moments of both the states can be reproduced accurately using an effective value of spin gyromagnetic ratio $(g_s)_{\text{eff}}=3.5$ and $g_R=Z/A$. The $B(E2)\uparrow$ value of the $\frac{5}{2}^+_1\rightarrow\frac{7}{2}^+_1$ transition deduced by Tanaka *et al.* has also been reproduced (Table VIII). The present calculation has reproduced quite closely the experimental spec-

TABLE V. Calculated and experimental quadrupole and magnetic moments.

			μ (μ_N)		Q (e b)	
A	I^π	E (keV)	Calc.	Expt.[a]	Calc.	Expt.[b]
^{149}Pm	$\frac{7}{2}^+$	0	+2.54	3.3(5)	+0.86	
	$\frac{5}{2}^+$	114	+3.07	+2.13(15), +2.40(30) 2.0(2),2.57(33)	+0.46	
	$\frac{3}{2}^+$	189	+2.35	2.25(6)	+0.56	
	$\frac{11}{2}^-$	240	+6.83		−1.0	
	$\frac{5}{2}^+$	211	+2.37	+2.20(35)	+0.98	
	$\frac{7}{2}^-$	270	+5.89	+2.19(11),3.6(2)	−0.69	
^{151}Eu	$\frac{5}{2}^+$	0	+3.52	+3.474(1)	+0.88	+0.90(1)
	$\frac{7}{2}^+$	22	+2.60	+2.591(2)	+0.99	+1.28(1)
	$\frac{11}{2}^-$	196	+6.85		−0.93	
^{153}Tb	$\frac{5}{2}^+$	0	+3.55		+0.89	
	$\frac{7}{2}^+$	80.7	+2.91		+0.72	
	$\frac{11}{2}^-$	163	+6.86		−0.83	

[a] Reference 17.
[b] Reference 20.

troscopic factors[18] for these two states as well as for two other $\frac{5}{2}^+$ states at 260 and 310 keV (Table IV). The correspondence between individual members in the calculated and experimental spectra (Fig. 6) can be made on the basis of their excitation energies and electromagnetic properties. The $B(E2)\uparrow$ values for a number of levels have been measured in the Coulomb excitation experiments.[4] It can be seen from Table VIII that the present work reproduces very closely the observed $B(E2)\uparrow$ values for most of the levels below 600 keV excitation energy. The notable exceptions are the observed $\frac{7}{2}^+$ and $\frac{9}{2}^+$ levels at 499 and 600 keV, respectively. The 600 keV ($\frac{9}{2}^+$) level has been identified by Taketani *et al.*[21] as a member of the rotational band based on the $\frac{5}{2}$[413] Nilsson level. In fact, the observed $\frac{5}{2}^+$, $\frac{7}{2}^+$, $\frac{9}{2}^+$, and $\frac{11}{2}^+$ levels at 260, 416, 600, and 845 keV, respectively, have been identified by them as the members of this band with the 260 keV ($\frac{5}{2}^+$) state forming the band head. In the Coulomb excitation work, the 260 keV ($\frac{5}{2}^+$) and the 414 keV ($\frac{7}{2}^+$) levels have not been excited. In the calculated spectrum, the $\frac{5}{2}^+$, $\frac{7}{2}^+$, $\frac{9}{2}^+$, and $\frac{11}{2}^+$ levels at 250, 443, 658, and 877 keV, respectively, receive appreciable contribution from the $\frac{5}{2}$[413] band in their wave functions. These levels can be identified with the corresponding members of the band proposed by Taketani *et al.* The calculated $B(E2)\uparrow$ strengths for these levels are found to be very small. One explanation for the observed appreciable $B(E2)\uparrow$ value for the 600 keV ($\frac{9}{2}^+$) level may be the mixed nature of

TABLE VI. Spherical shell model state admixtures for the Nilsson states included in the positive parity calculations. Also listed are the $\langle j^2 \rangle$ terms as calculated from Eq. (9b).

Nilsson state \ j	$\frac{1}{2}$	$\frac{3}{2}$	$\frac{5}{2}$	$\frac{7}{2}$	$\frac{9}{2}$	$\langle j^2 \rangle$
$\frac{1}{2}$[431]	0.09	0.19	0.20	0.48	0.04	11.48
$\frac{1}{2}$[420]	0.09	0.005	0.50	0.36	0.05	11.34
$\frac{1}{2}$[411]	0.17	0.54	0.15	0.13	0.01	5.73
$\frac{3}{2}$[422]		0.07	0.14	0.75	0.03	14.13
$\frac{3}{2}$[411]		0.01	0.76	0.20	0.03	10.61
$\frac{5}{2}$[413]			0.06	0.92	0.02	15.43
$\frac{5}{2}$[402]			0.91	0.07	0.01	9.46
$\frac{7}{2}$[404]				0.99	0.01	15.80

TABLE VII. Experimental and calculated energies and wave functions for the positive parity states in ^{153}Tb; contributions from the $\frac{1}{2}[431]$, $\frac{1}{2}[420]$, and the $\frac{1}{2}[411]$ Nilsson states were found to be very small except for the 743 keV ($\frac{9}{2}^+$) state and are omitted.

I^π	E (keV) Expt.[a]	Calc.	$\frac{3}{2}[422]$	$\frac{3}{2}[411]$	$\frac{5}{2}[413]$	$\frac{5}{2}[402]$	$\frac{7}{2}[404]$
$\frac{5}{2}^+$	0	0	0.008	0.431	0.060	0.897	
$\frac{5}{2}^+$	240.5	359	−0.147	−0.610	−0.679	0.351	
$\frac{5}{2}^+$	543.2[b]	474	0.125	−0.627	0.683	0.259	
$\frac{7}{2}^+$	80.7	90	0.069	0.338	0.337	0.542	0.685
$\frac{7}{2}^+$	254.2	221	−0.060	0.409	−0.246	0.639	−0.587
$\frac{7}{2}^+$	510[b]	543	0.184	0.596	0.572	−0.422	−0.276
$\frac{7}{2}^+$	740.7	701	0.193	−0.556	0.641	0.333	−0.318
$\frac{3}{2}^+$	147.5	238	0.013	0.985			
$\frac{9}{2}^+$	325.0	277	0.098	0.403	0.398	0.530	0.616
$\frac{9}{2}^+$	444.7	436	0.088	−0.442	0.328	−0.583	0.579
$\frac{9}{2}^+$	571.9	743	−0.259	−0.398	−0.478	0.316	0.364
$\frac{11}{2}^+$	529.4	493	0.125	0.436	0.444	0.505	0.575
$\frac{11}{2}^+$	630.6	668	−0.132	0.464	−0.376	0.546	−0.526
$\frac{13}{2}^+$	755.4	730	0.147	0.467	0.471	0.482	0.536
$\frac{13}{2}^+$	848.6	924	0.142	−0.486	0.414	−0.524	0.521
$\frac{15}{2}^+$	968.1	991	0.173	0.475	0.502	0.454	0.515
$\frac{15}{2}^+$	1067.1	1193	−0.184	0.500	−0.422	0.503	−0.449
$\frac{17}{2}^+$	1199.4	1266	0.186	0.496	0.517	0.435	0.485
$\frac{19}{2}^+$	1422.6	1563	−0.212	−0.490	−0.542	−0.410	−0.474
$\frac{21}{2}^+$	1681.6	1871	0.221	0.507	0.548	0.396	0.451
$\frac{23}{2}^+$	1923.8	2198	−0.246	−0.493	−0.571	−0.372	−0.445
$\frac{25}{2}^+$	2211.2	2535	0.249	0.509	0.571	0.314	0.426
$\frac{27}{2}^+$	2467.4	2889	−0.275	−0.489	−0.592	−0.341	−0.422

[a] Reference 2.

[b] No definite spin assignment is available from experimental data. These assignments have been made on the basis of the agreement between calculated and experimental excitation energies.

this state compared to that of the 260 keV ($\frac{5}{2}^+$) and 414 keV ($\frac{7}{2}^+$) members of the band. Another possibility is that the $\frac{9}{2}^+$ level at 600 keV observed by Taketani *et al.*[21] in their ^{152}Sm(2p,2nγ)^{151}Eu work and by Dracoulis *et al.*[4] in their Coulomb excitation work are not identical. The observed high spin positive parity levels ($\frac{11}{2}^+$, $\frac{13}{2}^+$, $\frac{15}{2}^+$, and $\frac{17}{2}^+$) have also been reproduced in the present work. The calculated wave functions show these levels to be mainly based on the $\frac{7}{2}[404]$ and $\frac{5}{2}[413]$ Nilsson orbitals. The present calculation fails to reproduce the observed spectroscopic factors of the $\frac{3}{2}^+$ levels. It is observed that the $\frac{3}{2}[402]$ Nilsson level which has a large contribution from the spherical $d_{3/2}$ shell model state lies at a very high excitation energy and has been excluded in the present calculation. Therefore the calculated $\frac{3}{2}^+$ levels receive contribution mainly from the $d_{5/2}$ and $g_{7/2}$ orbitals (Table VI) resulting in low spectroscopic strengths. From the Coulomb excitation experiment, it is seen that the $\frac{7}{2}^+$ state at 307.5 keV and the $\frac{9}{2}^+$ state at 503 keV have large $B(E2)\uparrow$ values. The calculated $\frac{7}{2}^+$ and $\frac{9}{2}^+$ state at 198 and 407 keV, respectively, have large admixture of the $\frac{5}{2}[402]$ band in their wave functions and the calculated $B(E2)\uparrow$ values are also very close to the experimental values for the $\frac{7}{2}^+$ and $\frac{9}{2}^+$ levels at 307.8 and 503 keV, respectively. These states have, therefore, been identified as high spin members of the band based on the $\frac{5}{2}[402]$ orbital. On similar considerations, the observed 307.8 keV ($\frac{9}{2}^+$) level and its theoretical counterpart, the $\frac{9}{2}^+$ level at 198 keV, can be considered as the member of a band based on the $\frac{7}{2}[404]$ level.

C. The nucleus ^{153}Tb

Available experimental data on the level properties of ^{153}Tb have recently been compiled by Lee.[2] A number of high spin states (both positive and negative parity) have been identified in this nucleus through (α,xn) reaction studies. Three normal positive parity band structures

TABLE VIII. Calculated and experimental $B(E2)\uparrow$ values for ^{151}Eu.

E (keV)	I^π	Expt.[a]	$B(E2)\uparrow$ (e^2b^2) Present work	Particle vibration coupling model[b]	Rotational model[a]
22	$\frac{7}{2}^+$	0.045	0.069	0.05	0.03
196	$\frac{3}{2}^+$	0.095	0.053	0.11	0.057
307.2	$\frac{5}{2}^+$	0.072	0.047	0.12	0.131
307.5	$\frac{7}{2}^+$	0.39	0.34	0.40	0.375
307.8	$\frac{9}{2}^+$	0.039	0.04	0.056	0.009
499	$\frac{7}{2}^+$	0.06	0.003	0.10	Very small
503	$\frac{9}{2}^+$	0.22	0.15	0.50	0.42
580	$\frac{5}{2}^+$[c]	0.015	0.018	0.021	
600	$\frac{9}{2}^+$	0.021	0.001		0.002
719	$\frac{7}{2}^+$[c]	0.028	0.015	0.009	

[a] Experimental results and the theoretical values calculated in a rotation particle coupling model are taken from Ref. 4 except for the measured $B(E2)\uparrow$ value for the 22 keV $\frac{7}{2}^+$ state which is taken from Ref. 20.

[b] Reference 1.

[c] No definite spin assignment is available from experimental data. These assignments have been made on the basis of the agreement between the calculated and experimental excitation energies and $B(E2)\uparrow$ values.

based on the $\frac{5}{2}$[402], $\frac{7}{2}$[404], and $\frac{3}{2}$[411] Nilsson orbitals and one Coriolis-decoupled $h_{11/2}$ related band have been tentatively proposed in this nucleus. The positive parity calculations were carried out with some adjustment of the single particle energies of the $\frac{7}{2}$[404] and $\frac{3}{2}$[411] orbitals to reproduce the low-energy part of the spectrum. The single-particle energies of these two states were adjusted by 200 and 400 keV, respectively. From the calcu-

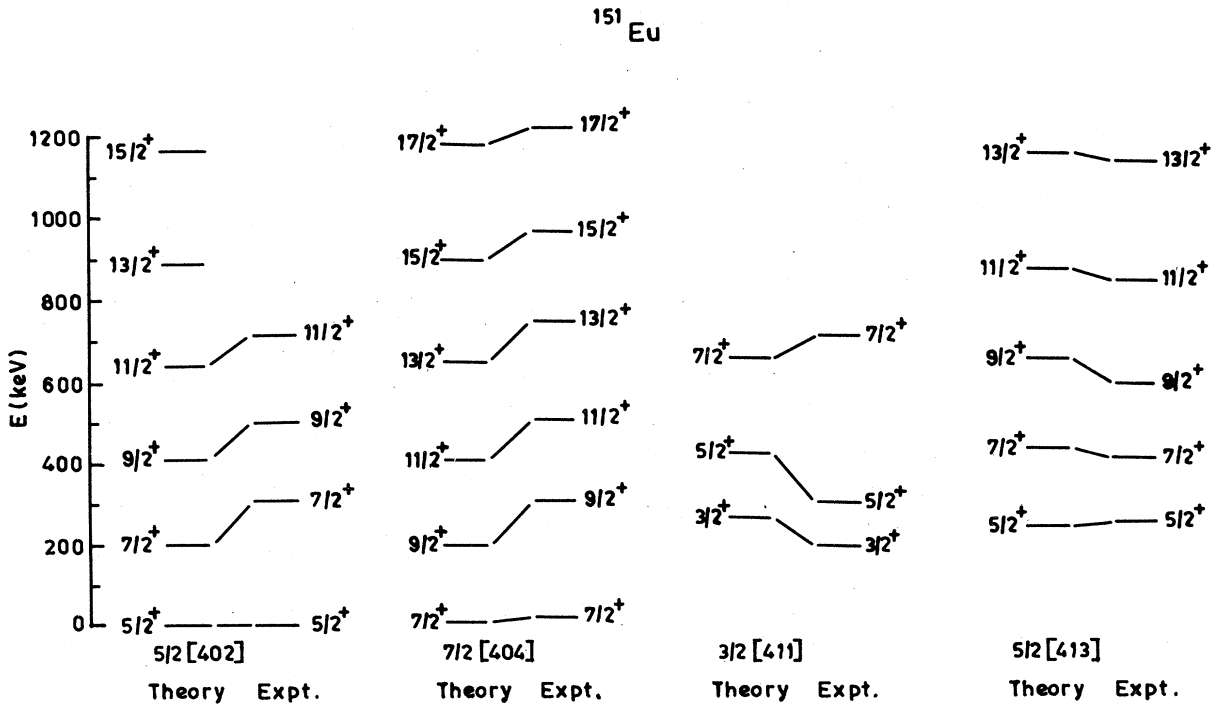

FIG. 6. Comparison of the experimental (Refs. 3–5, 16–18, and 21) and theoretical results for the positive parity bands based on $\frac{5}{2}$[402], $\frac{7}{2}$[404], $\frac{3}{2}$[411], and $\frac{5}{2}$[413] Nilsson orbitals in ^{151}Eu.

lated wave functions of the positive parity states (Table VII), it is seen that except for a few low-lying states, there is a significant amount of band mixing so that it is not easy to identify these states with particular bands. However, considering the largest components of their wave functions, two bands based on the $\frac{5}{2}[402]$ and $\frac{7}{2}[404]$ Nilsson orbitals can be identified in the calculated spectrum and the excitation energies of the band members are in close agreement with their experimental counterpart (Fig. 7). The band based on the $\frac{7}{2}[404]$ orbital is shown up to $J=\frac{17}{2}$ because the calculated wave functions of the higher spin states ($J>\frac{17}{2}$) indicate that they are highly mixed, the largest contribution coming from the $\frac{5}{2}[413]$ orbital. In the compilation of Lee,[2] these states have been shown as members of the band based on the $\frac{7}{2}[404]$ orbital. However, so far as the excitation energies of these states are concerned, agreement between the calculated and experimental data is not bad. The calculated $\frac{3}{2}^+$, $\frac{5}{2}^+$, and $\frac{7}{2}^+$ states at 238, 359, and 543 keV can be identified with the corresponding members of the proposed band based on the $\frac{3}{2}[411]$ orbital. The calculated excitation energies are systematically higher by about 100 keV than their experimental values.

The calculated spectroscopic strengths of some of the states ($\frac{5}{2}^+$, $\frac{7}{2}^+$, and $\frac{3}{2}^+$) are listed in Table IV and they are found to be in good agreement with corresponding experimental values, except for the $\frac{3}{2}^+$ states. Single-particle energies of Nilsson orbitals receiving large contribution from the spherical $d_{3/2}$ state come out to be very high except for the $\frac{1}{2}[411]$ orbital, and hence they have been excluded from our calculation. Therefore, the calculated spectroscopic factors for the $\frac{3}{2}^+$ states come out to be low.

Lifetimes of some of the levels and their decay modes have been calculated and compared with the experimental values (Table III). It appears that the present calculation is also successful in reproducing the electromagnetic properties of these levels.

VI. COMPARISON WITH OTHER THEORETICAL WORK

The level structures of these isotones have been studied by us previously in a version of the unified vibrational model incorporating both paring effects and anharmonicity in the core vibrations.[1] Pakkenen *et al.*[22] have reported briefly the results of their calculation of the level spectrum of ^{149}Pm in an axial particle rotor model where they could reproduce the majority of the levels below 600 keV. The ^{151}Eu has been studied by Dracoulis *et al.*[3,4] within the framework of a rotation-particle coupling model and

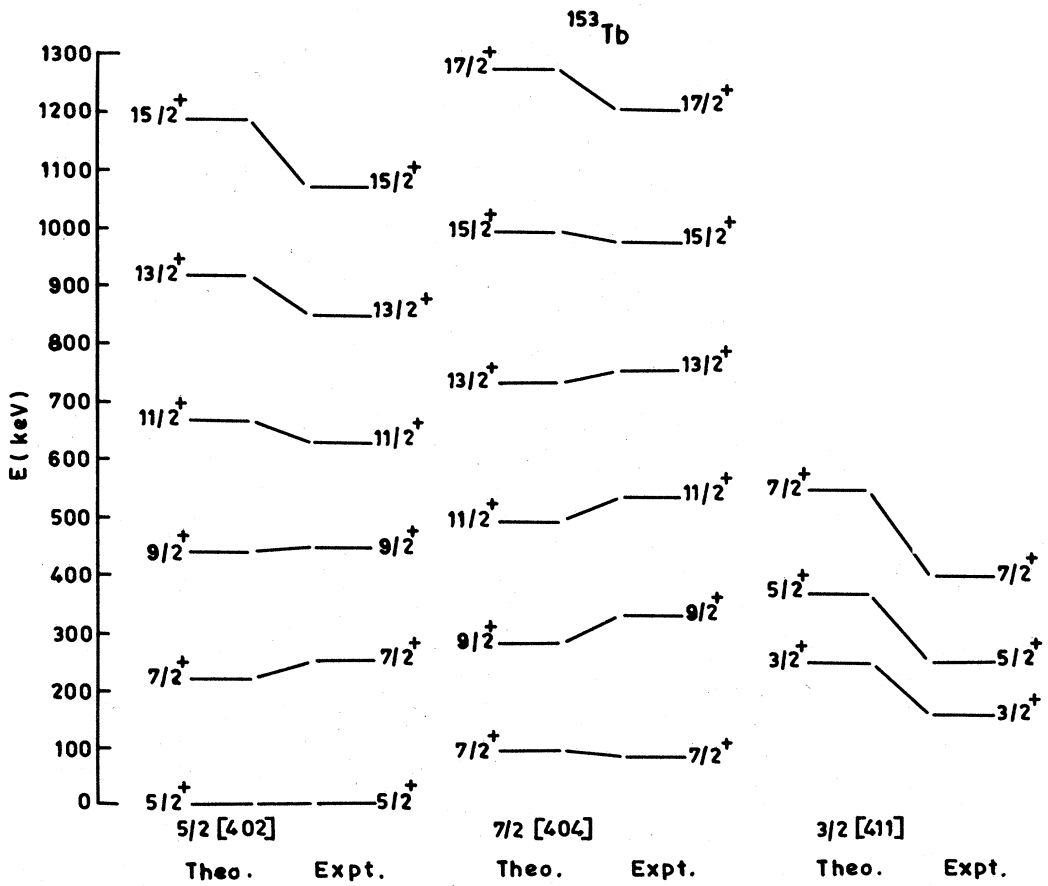

FIG. 7. Comparison of the experimental (Ref. 2) and theoretical results for the positive parity bands based on $\frac{5}{2}[402]$, $\frac{7}{2}[404]$, and $\frac{3}{2}[411]$ Nilsson orbitals in ^{153}Tb.

by Lo Bianco *et al.*[5] and Scholten and Blasi[6] in the interacting-boson-fermion model. The ^{153}Tb has been studied previously by Devous and Sugihara[23] in a particle plus rotor model with Coriolis mixing. However, so far no worker has reported any detailed and systematic study of these isotones within the framework of the same coupling scheme encompassing the high as well as low spin states and the electromagnetic properties of these levels. In ^{151}Eu and ^{153}Tb, it is found that the incorporation of the VMI approach has led to a much better agreement with the experimental spectra, especially for the high spin states compared to that obtained in conventional particle-rotor coupling model adopted by Dracoulis *et al.* and Devous and Sugihara. In ^{151}Eu, so far as the excitation energies of the members of different bands are concerned the present model and the interacting-boson-fermion model give comparable results. Since Scholten and Blasi and Lo Bianco did not report the results of their calculation of the electromagnetic properties of the excited levels, comparative study of these two approaches on this important structure property cannot be done. In ^{151}Eu, the $B(E2)\uparrow$ values for a number of levels are experimentally known and these can be used as a crucial test of the success of any theoretical model applied to this isotope. In ^{149}Pm, due to lack of sufficient experimental data, the results of the present as well as other calculations cannot be tested so rigorously. The quasiparticle anharmonic coupling approach adopted by us previously was successful in reproducing the majority of the experimentally observed levels in the low energy region in all the three isotones. However, the model failed to predict the observed high spin positive and negative parity states. Another remarkable success of that model was its ability to reproduce the observed spectroscopic strengths in the three isotones and almost all the observed $B(E2)\uparrow$ values in ^{151}Eu except for the 600 keV $\frac{9}{2}^+$ state. This is not surprising since these isotones lie in a transitional region and they, therefore, exhibit some characteristic features of both a vibrational and a rotational nucleus.

VII. CONCLUSION

A simple axially symmetric rotational model incorporating the ideas of the VMI approach was found to be successful in reproducing the properties of a number of transitional nuclei in the mass 70, 100, and 120 regions.[10] A similar approach has also been applied very recently to understand the properties of the odd mass Sm isotopes.[14] The present work shows that a large variety of experimental data on the level properties of the $N=88$ isotones ^{149}Pm, ^{151}Eu, and ^{153}Tb can be reproduced successfully within the framework of a similar approach. It is also found by comparing the results of the present work as well as that obtained in the interacting-boson-fermion model in ^{151}Eu that a symmetric rotor interpretation of this transitional nucleus is equally good, if not better than that of the latter approach. Obviously there are several shortcomings in the present approach. There are several parameters in this calculation and to some of them, proper physical significance cannot be assigned. The parameters C and $\mathcal{I}_{0K}$ used in this calculation cannot be considered as an elastic constant and a minimum moment of inertia as they are in the even-even case. These two quantities should be viewed simply as parameters which simulate the increasing trend of the moment of inertia with increasing nuclear spin as observed in the even-even nucleus. The calculations are done under the assumptions of a constant deformation δ ($=0.14$) which do not properly reflect the dynamic relationship of the deformation with increasing spin of a rotating nucleus. The most disturbing feature of the present calculation is the somewhat arbitrary choice of the parameters μ and κ. A sensible approach was to fix these parameters by imposing the condition that for zero deformation, the single particle energies of the orbitals $d_{5/2}$, $d_{3/2}$, $g_{7/2}$, $s_{1/2}$, and $h_{11/2}$ should correspond to those determined experimentally or otherwise in this region. It is found that $\mu=0.59$ and $\kappa=0.05$ give a reasonable agreement with the single-particle energies deduced by the fits of Reehal and Sorensen[13] to the energies and $B(E2)\uparrow$ values of the levels of the single-particle shell model nuclei in this mass region. However, the proton single particle energies deduced from the prescription of Reehal and Sorensen do not fully agree with those experimentally determined for the ^{146}Gd nucleus where the existence of $Z=64$ subshell closure has been experimentally demonstrated.[24] It is found that the energies of the Nilsson orbitals calculated with these values of μ and κ when used as input parameters fail to reproduce the low energy part of the experimental spectra in these isotones. The relative spacings of the relevant Nilsson orbitals also depend on the choice of δ. Moreover, although a value of hexadecapole deformation $\delta_4\simeq-0.04$ is suggested for well deformed nuclei in this region,[23] for simplicity we have considered only the quadrupole deformation. All these factors introduce some amount of uncertainty in the choice of μ and κ values. However, it is gratifying to note that this simple model with minor adjustments of a few parameters can reproduce the excitation energies, the spectroscopic strengths, and electromagnetic properties of a majority of the observed levels in these transitional nuclei. Since it has been found earlier that a quasiparticle anharmonic vibration coupling as well as boson-fermion coupling models are also able to reproduce a large amount of experimental data in these nuclei, it would be interesting to study the relationship, if there is any, between the Coriolis force and the particle vibration (or fermion-boson) coupling.[25] On the one hand the particle-vibration coupling plays an important role as one departs from sphericity, on the other, the Coriolis interaction assumes a dominant role as the deformation decreases towards sphericity. Study of this relationship may help to understand the nature of the transition from spherical to deformed shapes.

[1]R. K. Guchhait, S. Bhattacharya, and S. Sen, J. Phys. G 9, 631 (1983).
[2]M. A. Lee, Nucl. Data Sheets 37, 487 (1982).
[3]J. R. Leigh, G. D. Dracoulis, M. G. Slocombe, and J. O. Newton, J. Phys. G 3, 519 (1977).
[4]G. D. Dracoulis, J. R. Leigh, A. Johnston, and C. Garrett, J.

Phys. G **3**, 533 (1977).
[5]G. Lo Bianco, N. Molho, A. Moroni, A. Bracco, and N. Blasi, J. Phys. G **7**, 219 (1981).
[6]O. Scholten and N. Blasi, Nucl. Phys. **A380**, 509 (1982).
[7]M. A. J. Mariscotti, G. Scharff-Goldhaber, and B. Buck, Phys. Rev. **178**, 1864 (1969).
[8]A. B. Volkov, Phys. Lett. **41B**, 1 (1972).
[9]P. R. Gregory and T. Taylor, Phys. Lett. **41B**, 122 (1972).
[10]H. A. Smith, Jr. and F. A. Rickey, Phys. Rev. C **14**, 1946 (1976); P. C. Simms, F. A. Rickey, and R. K. Popli, Nucl. Phys. **A347**, 205 (1980).
[11]S. Bhattacharya, R. K. Guchhait, and S. Sen, in *Proceedings of the International Conference on Nuclear Physics, Florence, 1983* (Tipografia Compositori, Bologna, 1983), Vol. I, p. 156.
[12]A. Bohr and B. R. Mottelson, *Nuclear Structure* (Benjamin, New York, 1969), Vol. II.
[13]B. Reehal and R. Sorensen, Phys. Rev. C **2**, 819 (1970).
[14]K. Maki-Kuutti and E. Hammaren, Nucl. Phys. **A411**, 125 (1983).
[15]J. G. Fleissner, E. G. Funk, F. P. Venezia, and J. W. Mihelich, Phys. Rev. C **16**, 227 (1977).
[16]G. Lo Bianco, N. Molho, A. Moroni, S. Angins, N. Blasi, and A. Ferroro, J. Phys. G **5**, 697 (1979).
[17]*Table of Isotopes,* 7th ed., edited by C. M. Lederer and V. S. Shirley (Wiley, New York, 1978).
[18]O. Straume, G. Løvhøiden, and D. G. Burke, Nucl. Phys. **A266**, 390 (1976); O. Straume, G. Løvhøiden, D. G. Burke, and E. R. Flynn, Z. Phys. A **293**, 75 (1979).
[19]I. S. Lee, W. J. Jordan, J. V. Maher, R. Kamermans, J. W. Smits, and R. H. Siemssen, Nucl. Phys. **A371**, 111 (1981).
[20]Y. Tanaka, R. M. Steffen, E. B. Shera, W. Reuter, M. V. Hoehn, and J. D. Zumbro, Phys. Rev. C **29**, 1897 (1984).
[21]H. Taketani, M. Adachi, T. Hattori, T. Matsuzaki, and H. Nakayama, Phys. Lett. **63B**, 154 (1976).
[22]A. Pakkenen, M. Kortelahti, M. Piiparinen, E. Hammerin, T. Komppa, and R. Komu, *Structure of Medium Heavy Nuclei, 1979,* Inst. Phys. Conf. Ser. 49 (The Institute of Physics, London, 1979), p. 301.
[23]M. D. Devous, Sr. and T. T. Sugihara, Phys. Rev. C **15**, 740 (1977).
[24]K. S. Toth, D. M. Moltz, E. C. Schloemer, M. D. Cable, F. T. Avignone III, and Y. A. Ellis-Akovali, Phys. Rev. C **30**, 712 (1984).
[25]T. L. Khoo, Nucl. Phys. **A347**, 407 (1980).